

TIME-DEPENDENT EARTHQUAKE RISK FOR REGIONAL RESILIENCE

David LALLEMANT¹, Anirudh RAO² and Anne KIREMIDJIAN³

Abstract: Earthquake risk and resiliency are dependent on time varying processes that are most frequently ignored in the models used to estimate. In this paper, a framework for a dynamic risk model is presented that includes time dependent (a) earthquake occurrence model, (b) fragility function development for deteriorating structures exposed to different environmental conditions, and (c) fragility functions that change in floor plan and increase in number of stories over time. The effects of time dependence on the overall risk are studied through a series of examples. It is found that the risk changes significantly with increased time since the last major earthquake event. Similarly, the vulnerability of structures depends on the environmental conditions that influence corrosion rates and buildings become increasingly more fragile as the number of stories or floor plans increase. Growth of building stock due to population growth further increases the risk and increase challenges for creating resilient communities.

Introduction

Earthquake resilience depends on many factors including the exposure of a region to various size earthquakes, the vulnerability of the built environment to these earthquakes and the financial, professional and labour capacity of the region to recover from such events in a timely manner. The assessment of the regional risk to potential earthquakes is a key component in this process. Over the past several decades many methods have been developed to estimate that risk in terms of financial losses, down time losses and casualties. These risk estimates typically assume that the earthquake events occur independently in time and homogeneously in space. In addition, the state of infrastructure is assumed to be in its as-built condition, and future exposure is assessed by the present-day building and other infrastructure inventory. Most frequently, the time value of money is also disregarded in future loss forecasts.

The risk assessment process should include all components that are time varying casting it in a dynamic model. While it is appropriate to model small to moderate earthquake occurrences as time independent and space homogeneous events, large infrequent earthquakes that rupture segments of tectonic features known as seismic gaps, are neither time dependent nor space homogeneous. Thus, earthquake occurrences models for large events need to reflect their time and space-dependent characteristics.

The second component that requires consideration of time is the fragility modelling of various structures. Presently, simple modifications are often introduced to account for the age of the structure and as a result reflect different earthquake resistant design criteria, however, the actual deterioration that structures undergo over their life due to variety of environmental factors are often ignored. Such deterioration is dependent both on time since construction as well as on the exposure of the structure to different environmental conditions such as dry vs. humid or areas with severe icing.

When estimating the risk to a region, we again consider the inventory of buildings that is currently in place. Analysis based on these inventories reflects current risk and does not take

¹ PHD Candidate, Stanford University, Stanford, CA, d.lallemant@gmail.com

² Research Engineer, Global Earthquake Model Consortium, Pavia, Italy, rao.anirudh@gmail.com

³ Professor of Civil and Environmental Engineering, Stanford University, Stanford, CA, ask@stanford.edu

into consideration urban or suburban growth, as well as population migrations. Changes in inventory can be due to new construction, increases in floor area of existing buildings (horizontal growth) or increases in number of stories of existing buildings (vertical growth). When forecasting future losses it is important to understand changes in structural characteristics and building inventory over time.

In this paper, a framework for a dynamic risk assessment is presented that includes time dependent earthquake occurrence modelling, fragility function development for (a) deteriorating structures exposed to different environmental conditions, (b) fragility functions that change in floor plan over time, and (c) fragility functions that increase vertically. Recent studies by Rao et al. (2014) have shown that the fragility of reinforced concrete bridge piers are significantly different when they are located immediately in the splash zone and those that are some distance away from the coastline. Similarly, studies by Lallemand et al. (2014) show dramatic increase in building fragility with increases in building height for in-filled masonry structures. Applications of these studies to various regions also demonstrate the increase in losses with time due to increased vulnerability.

We first summarise the dynamic risk framework presenting formulations for the different time-dependent components. Example applications show (a) the effect of corrosion on bridge columns depending on their environmental exposure and (b) the effect of increases in building stock in regions with predominantly masonry infill constructions, which is widely used in developing countries in the world.

Dynamic Earthquake Risk Framework

The performance-based earthquake engineering methodology (PBEE) that has been formulated in the past decade (e.g., Cornell & Krawinkler 2000, Krawinkler & Miranda 2004) is now widely accepted as the approach to evaluate the risk to individual structures. The fundamental assumption in this methodology is that the earthquake hazard can be modeled as a Poisson process and fragility functions are for structures in their as-built conditions.

In the present paper, we use the PEER performance based equation to formulate the dynamic earthquake risk framework. The time-dependent components within this framework are first identified and then methods for treating these components are presented. The original PEER performance based equation is given as follows:

$$\lambda_{DV}(dv) = \iiint G_{DV|DM}(dv|dm) |dG_{DM|EDP}(dm|edp)|^* |dG_{EDP|IM}(edp|im)|^* d\lambda_{IM}(im) \quad (1)$$

where $\lambda_{DV}(dv)$ is the annual rate of exceeding a decision variable DV , DM is the damage measure, EDP is the engineering demand parameter, IM is the intensity measure, $\lambda_{IM}(im)$ is the hazard rate and $|G(*)|$ is the absolute value of the complementary cumulative probability distribution.

The components in Equation 1 that are dependent on time are the hazard rate, structural demand and capacity, and value of money. The hazard rate, $\lambda_{IM}(im)$, in Equation 1 is only a function of IM and not of time. For large event, this function will depend on the time, t , since the last earthquake occurrence thus we denote it as $h_{IM,T}(im,t)$. The fragility of structures is evaluated by considering the demand, denoted as EDP , and their capacity defined in terms of a damage measure, DM . Both of these variables depend on the state of the state of the structure. Two types of temporal changes in structural characteristics are included in the formulation. The first estimates the degree of deterioration due to corrosion that depends on environmental exposure since initial construction. The second considers the changes in building as floors areas are expanded in plan or by adding stories to an existing structure. These dynamic changes in structural fragility are modelled through a time dependent variable W and its corresponding time dependent probability density function, $f_W(w,t)$.

Equation 1 for the likelihood of exceeding of a decision variable DV in a small increment of time given that the last major event occurred in time $(0,t)$ is now written in terms of the change in the structural demand or capacity given W and the time dependent hazard rate as shown in Equation 2:

$$\lambda_{DV,k}(dv, t) = \int_w \int_{im} \int_{edp} \int_{dm} G_{DV|DM,k}(dv | dm) dG_{DM|EDP,k}(dm | edp, w) dG_{EDP|IM,k}(edp | im, w) f_{vk}(w, t) dh_{IM,k}(im, t) dw \quad (2)$$

where the complimentary probability distributions of DM and EDP are now functions of the change W that reflects either deterioration level of building configuration at the time of the analysis.

Time-Dependent Seismic Hazard

For time-dependent events the time to the next event given the time of occurrence of the last event is modeled as a random variable with an interarrival probability distribution, $f_T(t)$, where t is the time since the last event. The hazard rate, $h_T(t)$, is then

$$h_k(t) = \frac{f_k(t)}{1 - F_k(t)} \quad (3)$$

where $F_T(t)$ is the cumulative distribution function of the time since the last event. For Poisson processes the hazard rate is constant. For time dependent events, the hazard rate should increase with time. Probability models that have been used previously for the earthquake interarrival times include the exponential (time-independent), Weibull, lognormal and Brownian Passage Time (BPT) distributions (for time-dependent events).

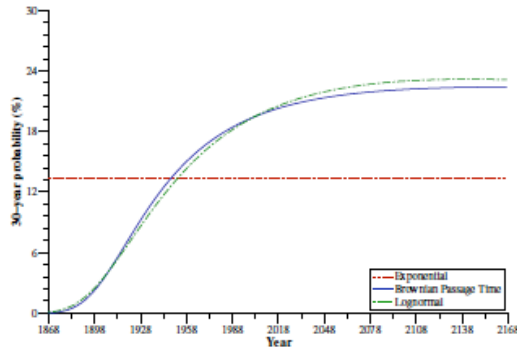


Figure 1. Comparison of earthquake hazard rate for the south Hayward fault with different interarrival time distributions.

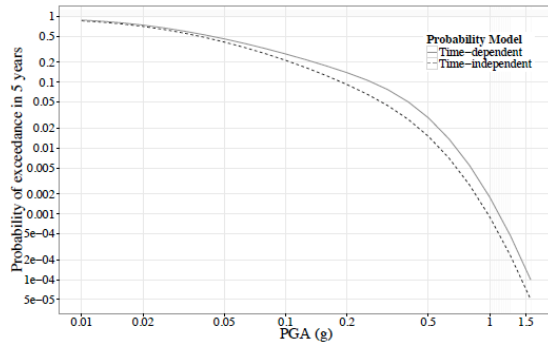


Figure 2. Comparison of time-independent and time-dependent 5-year PGA hazard curve for Oakland CA.

Figure 1 shows the change in hazard rate for the Hayward fault where the last event is known to have occurred in 1868 and the average time between events is estimated to be 210 years with coefficient of variation of 0.6 (Parsons 2008). Figure 2 shows the effect of time dependence on the probabilities of exceeding peak ground acceleration (PGA) in units of g for the time dependent and time independent models. As can be seen from Figure 2 the Poisson model underestimates the hazard once the mean interarrival time has been reached or is exceeded.

Seismic Fragility Functions for Deteriorating Structural Components

Over their lives, structures deteriorate due to variety of causes. Deterioration in bridge columns in particular is due to corrosion, scour, freeze-thaw attacks, creep, and fatigue caused by load history. Long-term structural deterioration may greatly increase the vulnerability of a bridge to earthquake loads due to reduced structural capacity. Rao et al. (2014) provide an extensive review of previous work on deteriorating structures due to corrosion and propose a model for deterioration dependent fragility function development. In this paper, their formulation is adopted and only briefly summarized.

To account for structural deterioration effect in damage state capacities and seismic demand on the structure, Rao et al. (2014) introduce an intermediate variable called the deterioration measure, W . As an example, for chloride-induced reinforcement corrosion deterioration, possible alternatives for W might include (i) proportion of reinforcement steel mass lost, which is commonly denoted as X , (ii) maximum pit depth, if pitting corrosion were observed, and (iii) amount of concrete cover lost due to cracking and spalling. Corrosion of reinforcement damages concrete structures in multiple ways. The area of both longitudinal and transverse steel is reduced due to the formation of rust. The reduction in steel cross section can be due to uniform corrosion or pitting corrosion. With uniform corrosion the reduction in cross section of all rebar in the perimeter of the column is assumed to be the same. Cracking of the concrete cover usually follows the increase in corrosion deposit. Pitting corrosion occurs when the concrete cover cracks leading to corrosion concentrating at particular locations. The localized reduction in steel cross-section causes localized strain peaks in the steel reducing its ductility. Concrete cover cracking and spalling may lead to a reduction in the concrete cross-sectional area. Bond-strength reduction between steel and concrete may also occur. These events can lead to reduction in yield and ultimate strength in the reinforcing bars, and buckling.

An analytical model for a non-corroded bridge column was developed using the Open System for Earthquake Engineering Simulation (OpenSees) software. The column was modelled as a nonlinear distributed-plasticity, fibre beam-column element, which is a flexibility-based element that considers the spread of plasticity along the length of the member. The details of the model are given in Rao (2014). Two tests data were used to validate the structural model for the corroded columns (State Key Laboratory of Coastal and Offshore Engineering at Dalian University of Technology in China, Li and Gong 2008); the Newmark Structural Engineering Research Laboratory of the Department of Civil and Environmental Engineering at University of Illinois at Urbana-Champaign, Aquino 2002; Aquino & Hawkins 2007). Using these tests, it is shown that the simplest of the analytical corrosion models provides the same degree of accuracy as the model proposed by Berry and Eberhard (2006) for non-corroded columns.

A probabilistic formulation for the time to corrosion initiation, the rate of corrosion, and the time to cover cracking after corrosion initiation to capture their uncertainty was developed by Rao (2014) and summarized in Rao et al (2014). The formulation was tested with three columns built respectively in the 1960's, 1980's and the 2000's reflecting varying seismic design requirements and degrees of deterioration. These columns are referred as to C_{60} , C_{80} and C_{00} . In order to capture exposure to varying environmental conditions, the three columns are placed within (a) the coastal splash zone and (b) the coastal and marine atmosphere zone (distance to the coastline $d_{coas} = 200$ m). In the splash zone the columns are subjected to direct salt spray from the tidal water and have high concentration of chlorides on the surface with a mean of 7.35kg/m^3 and coefficient of variation (COV) of 0.7 of surface chloride concentration (after Val and Stewart, 2003).

The demand curves for the non-corroded columns are obtained first and then column deterioration is incorporated to reflect the degree of mass loss due to corrosion. For this paper the IM selected is the peak ground acceleration, PGA . The engineering demand parameter, EDP , is set at as the maximum drift ratio. A set of 40 ground motions for rock sites was used to simulate the demand on the column. To account for the deterioration effect of corrosion in the column the following changes are made for the degree of corrosion: (a) the area of the longitudinal reinforcing steel is reduced and (b) the strength of the cover concrete elements is reduced. The change in bond strength with corrosion was not considered in the analysis. Figures 3a and 3b show the effect of environmental exposure on the degree of corrosion $X(t)$ for the C_{60} column.

Table 1 provides the definitions used in this study. With these definitions of damage state, analytical formations are used to correlate the column median value of maximum drift ratio to observed damage (see Rao 2014). The coefficients of variation used in the analysis are those proposed by Berry and Eberhard (2006) and Mackie et al. (2008). The material and

geometric properties of the non-corroded columns are changed to represent the degree of corrosion. The changes in fragility functions with increase in degree of corrosion are shown in Figure 4 for 0% to 40% of mass loss in increments of 10% for damage state 4. Lognormal distributions are fitted to the capacity fragility functions as shown in Figure 4 for the C₆₀ column.

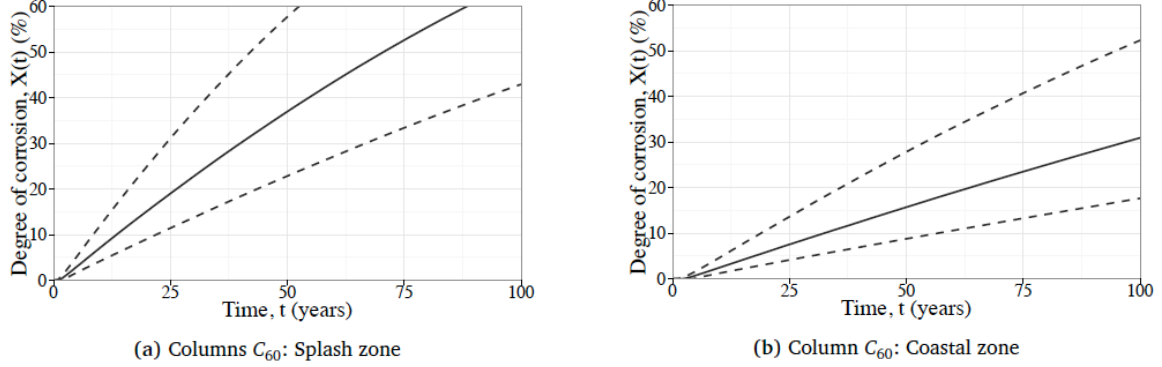


Figure 3. Degree of column deterioration (% steel mass loss for the C60 column in (a) the splash zone and (b) the coastal/marine atmospheric zone.

Table 1. Bridge column damage states descriptions

Damage State	Description	Repair
D1: Slight	Minor cracks	Seal cracks and paint
D2: Moderate	Shear cracks and spalling	Epoxy injection and spall repair
D3: Extensive	Bar buckling	Replace buckled bars and FRP wrap
D4: Complete	Collapse or imminent collapse	Replace column

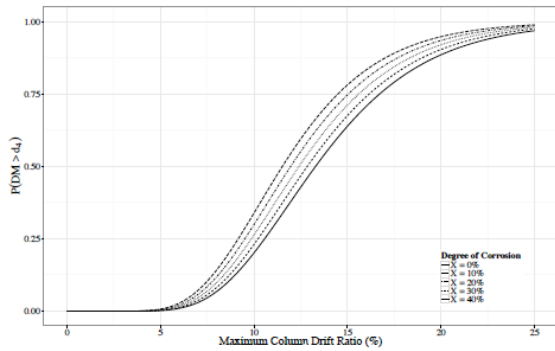


Figure 4. Variation of capacity curves with increasing mass loss for damage state 4 for the C₆₀ columns.

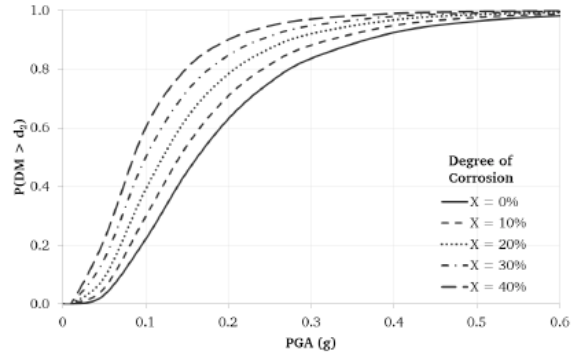


Figure 5. Fragility curves for the C₆₀ column for damage state D2 as functions of increased corrosion.

With the median and dispersion of damage state capacities and the median and dispersion of the demand at various intensity levels evaluated, the fragility for the four damage states for the non-corroded and corroded columns can be obtained by integrating the two functions. The probability of being or exceeding a specified damage state *i* that includes the effect of corrosion is given by

$$F_k(im, w) = P_{NC|w}(im | w) * \Phi \left[\frac{\mu_{\ln D(im, w)|NC} - \mu_{\ln C_i(w)}}{\sqrt{\beta_{D(im, w)|NC}^2 + \beta_{C_i(w)}^2}} \right] + P_C(im, w) \quad (4)$$

where $\mu_{\ln D(im)|NC}$ = mean of the natural logarithm of the seismic demand at intensity level *im* given that there is no collapse (NC); $\mu_{\ln C_i}$ = mean of the natural logarithm of the *i*th damage state capacity; β corresponds to the logarithmic standard deviations of capacity and demand; *w* = degree of mass loss; $P_{NC}(im)$ and $P_C(im)$ are respectively the probabilities of no collapse

and collapse. Figures 5 show the fragility functions for the C_{60} column with increasing levels of corrosion for DS 2.

Seismic Fragilities for Incremental Construction with Time

In order to conduct time-dependent large-scale risk assessment, incremental construction as a significant cause of changes in vulnerability, as well as changing building practices (due to changes in building code, its enforcement, material quality or other), is considered in addition to structural deterioration. In rapidly urbanizing cities, the pay-as-you-go process of informal building construction and expansion is the de facto pattern of growth. Indeed the informal sector builds an estimated 70% of all urban housing in developing countries (Goethert 2010). This process starts with a simple shelter and, given enough resources and time, transforms incrementally to multi-story homes and rental units. However no robust studies have investigated the effect of these incremental expansions on vulnerability, particularly to seismic hazards.

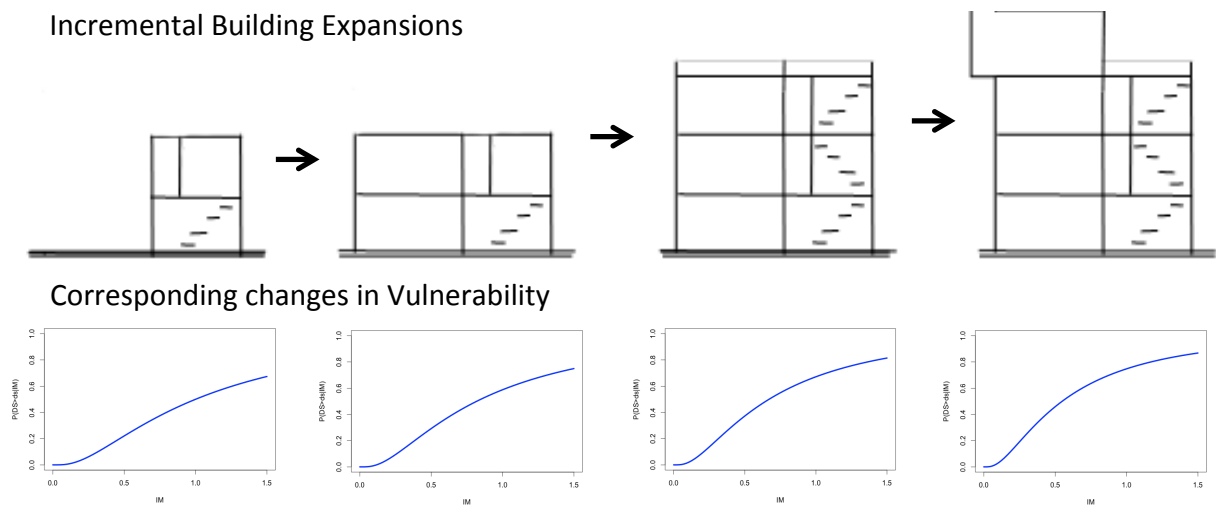


Figure 6. Diagram of the process of incremental building construction typical of cities throughout the world, and corresponding hypothetical fragility curves reflecting the fact that vulnerability tends to increase with additional floors and discontinuous expansions.

The proposed framework defines typical stages within building evolution, and associated earthquake fragility curves reflecting the changes in vulnerability induced by each building expansion. Alternatively, these increments can be linked not to new fragility curves, but can be treated as additional vulnerability indicators in multivariate fragility models.

Case Study of Loss for Deteriorating Single Column

Figure 7 shows the variation in annual loss and standard deviation in annual loss as functions of the degree of deterioration W for the three columns described previously. These figures illustrate the large difference in expected losses between the different columns. While the difference is small between the C_{80} and C_{00} column, the C_{60} column has expected losses that are almost four times larger than the C_{00} and almost twice than the C_{80} . This highlights the fact that neglecting the effects of deterioration for the older bridge columns could lead to a severe underestimation of potential losses.

The effect of environmental conditions is shown in Figure 8. The expected annual losses for columns in the splash zone are significantly higher than those in the coastal zone. That difference is the highest for the C_{60} column, as expected and smallest for the C_{00} column reflecting the greater concrete cover in the C_{00} column that results in lower corrosion rates.

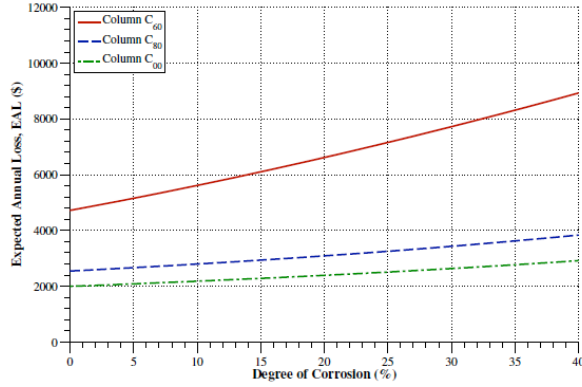


Figure 7. Expected annual loss given W for Columns C₆₀, C₈₀ and C₀₀.

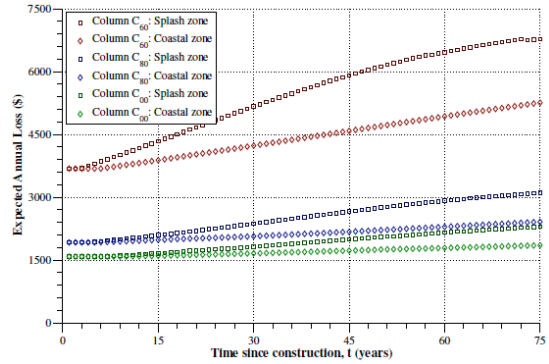


Figure 8. Expected annual loss for Columns C₆₀, C₈₀, C₀₀.

Case Study of Damage Estimates to Kathmandu, Nepal

The framework described above was applied in order to forecast the earthquake risk of Kathmandu city in Nepal. Since the main interest is to capture changing risk driven by time-dependent exposure and vulnerability, the study describes the risk at several times based on a single scenario: a reproduction of the 8.1 magnitude Bihar earthquake of 1934. This example demonstrates a simplified application of the framework described, based on very limited data and simple models. The results themselves are therefore not aimed at accuracy of risk forecasting but simply to demonstrate the importance of including urban dynamics in risk assessment of cities.

Spatially correlated ground motion fields for peak ground acceleration were generated based on Jayaram and Baker’s (2009) correlation model applied with the Chiou and Young (2008) ground motion prediction equation. Four exposure models were used in this study. Census data for population was obtained for years 1991 and 2001. No census data was available for more recent years. The population for years 2010 and 2020 were therefore projected based on a simple compounded annual growth rate:

$$pop(t) = (pop(t_1) / pop(t_0))^{(t-t_0)} \times pop(t_0) \quad (5)$$

where $pop(t)$ is the population at time t , and t_1 and t_0 are the two time instances for which data are available. The census data are available at the “ward” level. Since the spatial resolution of the ward-level census data is larger than the ground motion correlation distance, such aggregated data would result in overestimating extreme losses. This is because the probability of any single site having large ground motion is higher than for numerous dispersed sites. Hence aggregating entire ward exposure at its centroid could amplify the probability of extreme loss. For this reason the population data was spatially interpolated on a 500m x 500m grid.

The population data was converted to a building inventory based on the 2001 census, which provides the number of buildings for each ward as well as a distribution of buildings within five categories: (1) stone with mud mortar, (2) adobe with mud mortar, (3) brick with mud mortar, (4) brick with cement mortar, and (5) reinforced concrete frame with masonry infill as shown in Figure. Since the majority of new construction is reinforced concrete frames with masonry infill, the ratio of this building type increases with time.

Fragility curves for each of these building types were obtained from a previous study which calibrated fragility curves based on the 1988 Udayapur earthquake damage assessment JICA (2002). This study provided for each building a vulnerability curve describing the damage ratio given peak ground acceleration, and a fragility curve of “heavy damage or collapse” given peak ground acceleration. For simplicity, we look at rates and distribution of “heavy damage or collapse” as a metric to measure time-varying risk.

Figure shows the distribution of the number of heavily damaged or collapsed buildings for each of the four exposure models, based on the same ground motion field simulation. The

results clearly show significant changes in risk driven by urban growth patterns and changes in primary construction type.






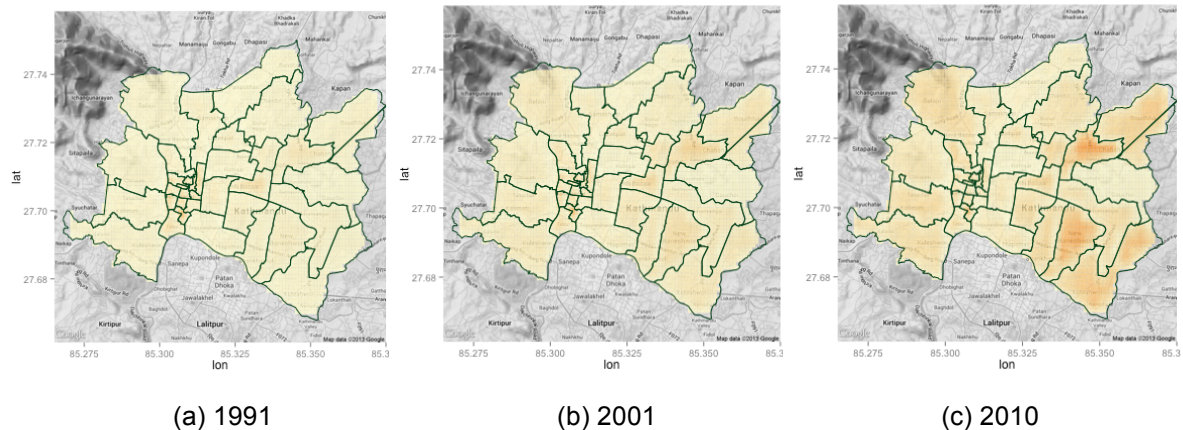
<i>Stone + mud mortar (ST) (5%)</i>	<i>Adobe (AD) (19%)</i>	<i>Brick + mud mortar (BM) (27%)</i>
		
<i>Popular in rural areas, round riverbed rocks and squared dressed stones</i>	<i>Old type of building composed of sun-dried bricks with mud mortar mainly in rural areas, can be found in old urban or sub-urban areas, mainly on elevated ground</i>	<i>Traditional style with burned bricks using timber on the floor or / and roofs, usually.</i>
<i>Brick + cement mortar (BC) (26%)</i>	<i>RC + masonry (RC) (23%)</i>	
		
Cement and Sand have become popularly used in last 30 years. BC becomes popular structure.	RC has been adopted in the last 20 –30 years. Vulnerable higher stories become popular.	

Figure 10. Pictures of five building types described in 2001 census. Credit to Segawa et al. 2002. The changing risk reflects both the high growth rates of specific wards, as well as the distribution/re-distribution of vulnerable building types. However, the absolute values of damage are not only emblematic of changing risk, since the maps are generated from a single ground motion field. Therefore the east side of the city sustains heavier damage in part as a result of higher ground motions from this specific simulation shown in Figure 11(e). The results demonstrate that changes in exposure and vulnerability in Kathmandu drive a significant increase in risk. The expected number of buildings sustaining heavy damage or collapsing (mean values shown in **Error! Reference source not found.**) nearly double every 10 years. Furthermore, the spread of the probability distribution of damage also increases. This increase is most likely the result of increased concentration of exposure. Indeed there is a higher probability of “tail events” (extreme damage or little damage) if sites of spatially concentrated exposure are within the spatial correlation length of ground motion intensity, as occurs with significant population growth.



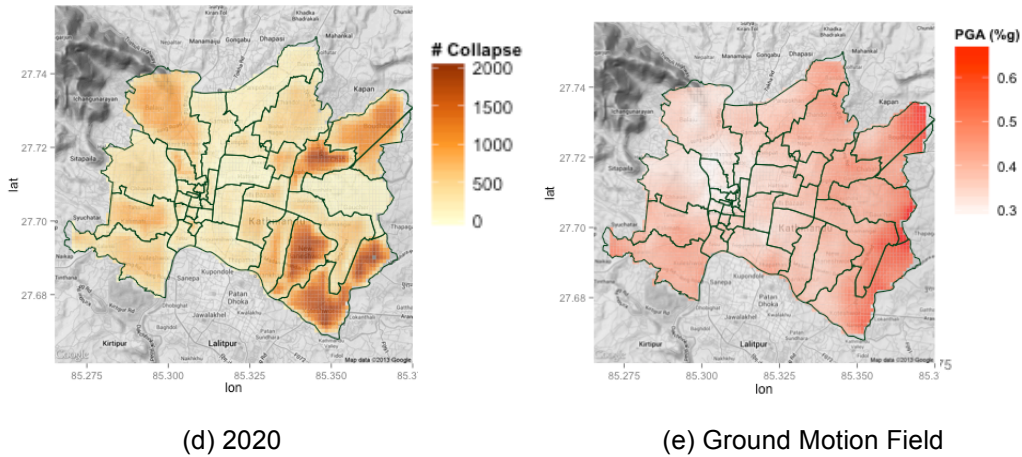


Figure 11. Number of buildings sustaining heavy damage or collapse for (a) 1991, (b) 2001, (c) 2010 (projected), (d) 2020 (projected) from a single ground motion field (e).

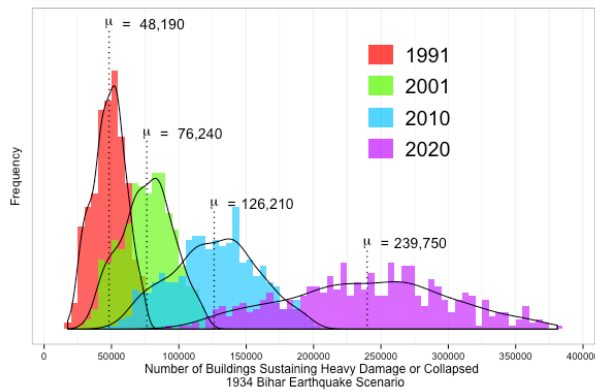


Figure 12. Full distribution of the number of buildings sustaining heavy damage or collapse, for four different time frames.

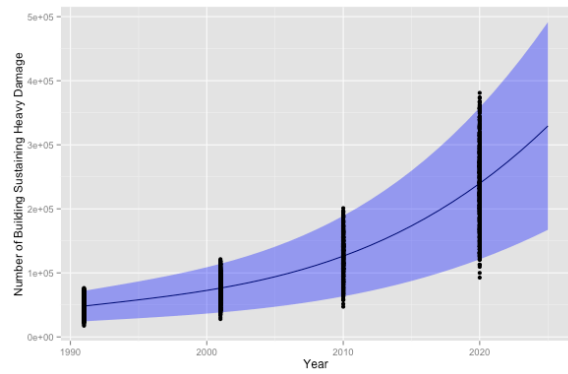


Figure 13. Expected and confidence interval of number of buildings sustaining heavy damage or collapse as function of time.

Conclusions

This study proposes a framework for assessing time-dependent seismic risk. In particular, it enables the inclusion of dynamic exposure and vulnerability models in order to forecast future losses from earthquakes. The basic framework described can be applied for various levels of data availability and resolution. For component-level analysis, the deterioration in bridge columns is investigated under different environmental exposure and thus on the rate of deterioration. It is found that losses due to deterioration are dependent on the corrosion rate, which is influenced by the exposure environment. Losses from bridge columns located in the splash zone are considerably larger than those at coastal areas away from the splash zone demonstrating the importance of deterioration rate. Although not included in the paper, it is also shown (Rao 2014 and Rao et al. 2014) that the consideration of time dependent hazard has important implications to the risk estimates. The spatial and temporal dynamics of urban exposure change can be modeled separately and included in the model through a single time-dependent parameter of exposure. The study further demonstrates an application of the time-dependent seismic risk framework to a data-sparse context of Kathmandu in Nepal. Results show a very significant increase in seismic risk as a result of increases in exposure and the redistribution of building among various types. Further studies will look at adding further complexity to this model, including more realistic urban growth models, time-varying vulnerability linked with incremental construction, and capturing risk related to secondary seismic hazards such as liquefaction and landslides. Of particular importance is that by focusing on modeling future risk, the framework enables the investigation of risk consequences from various policy and planning decisions.

Acknowledgements

The research presented in this paper was partially supported through an NSF Grant CMMI-106756 and NEESR-105651. We also thank the Global Fund for Disaster Reduction and Recovery (GFDRR) for their support.

REFERENCES

- Aquino, W and Hawkins, N M 2007. Seismic Retrofitting of Corroded Reinforced Concrete Columns Using Carbon Composites. *ACI Structural Journal*, 104(3):348–356,
- Aquino, W. 2002. Long-Term Performance of Seismically Rehabilitated Corrosion-Damaged Columns. Ph.d. dissertation, University of Illinois at Urbana-Champaign.
- Berry, M P and Eberhard, M O 2006. Performance modelling strategies for modern reinforced concrete bridge columns. Technical report, Pacific Earthquake Engineering Research Center, University of California, Berkeley, Berkeley, CA
- Chiou B-J and Youngs RR. 2008. An NGA Model for the Average Horizontal Component of Peak Ground Motion and Response Spectra. *Earthquake Spectra*. 24(1):173–215.
- Choe, D-E, Gardoni, P, Rosowsky, D V and Haukaas, T 2008. Probabilistic capacity models and seismic fragility estimates for RC columns subject to corrosion. *Reliability Engineering & System Safety*, 93(3):383–393
- Cornell, C A and Krawinkler, H 2000. Progress and Challenges in Seismic Performance Assessment. *PEER Center News*, 3(2):1–4
- Goethert R. 2010. Incremental Housing. *Monday Developments*.
- Japan International Cooperation Agency (JICA). 2002. *The Study on Earthquake Disaster Mitigation in the Kathmandu Valley Kingdom of Nepal*:1–161.
- Jayaram N and Baker JW. 2009. Correlation model for spatially distributed ground-motion intensities. *Earthquake Engineering & Structural Dynamics*.
- Krawinkler, H. and Miranda, E. 2004. Performance-based earthquake engineering. In Y. Bozorgnia & V. V. Bertero, ed., *Earthquake Engineering: From Engineering Seismology to Performance-Based Engineering*, Ch.9. CRC Press LLC, Boca Raton, FL
- Lallemand D, Wong S, Morales K and Kiremidjian A, 2014. A Framework and Case Study for Dynamic Urban Risk Assessment. *Proceedings of the 10th National Conference in Earthquake Engineering*, Earthquake Engineering Research Institute, Anchorage, AK.
- Li, J and Gong, J 2008. Influences of Rebar Corrosion on Seismic Behavior of Circular RC Columns. *China Journal of Highway and Transport*, 21(4):55–60
- Mackie, K R, Wong, J-M and Stojadinovic, B 2008. Integrated Probabilistic Performance- Based Evaluation of Benchmark Reinforced Concrete Bridges. Technical Report, January, Pacific Earthquake Engineering Research Center, University of California, Berkeley, Berkeley, CA
- Parsons, T. 2008. Earthquake recurrence on the south Hayward fault is most consistent with a time dependent, renewal process. *Geophysical Research Letters*, 35(L21301)
- Rao A, Lepech M, Kiremidjian A (2015). Time-Dependent Earthquake Risk Assessment Modeling Including Sustainability Metrics, *Journal of Structure and Infrastructure Engineering, Special Issue on Life-Cycle Civil Engineering*, under review.
- Rao, A. 2014. Structural Deterioration and Time –Dependent Seismic Risk Analysis, PhD. Dissertation, Stanford University, Stanford, CA
- Segawa S, Kaneko F, Ohsumi T and Hayashi H. 2002. Earthquake Damage Assessment in the Kathmandu Valley and its Application. ASC 2002, *Symposium on Seismic Earthquake Hazard Assessment & Risk Management*, 24-26 Nov. 2002, Kathmandu, Nepal:1–10.
- Val D. V. and Stewart M. G. 2003. Life-cycle cost analysis of reinforced concrete structures in marine environments. *Structural Safety*, 25(4):343–362
- Zhang, J., Gardoni, P. and Rosowsky D. V. 2012. Seismic fragility estimates for corroding reinforced concrete bridges. *Structure and Infrastructure Engineering*, 8(1):55–70.